Arginase-Negative Mutants of Arabidopsis Exhibit Increased Nitric Oxide Signaling in Root Development[1][W][OA]

Teresita Flores[2,3], Christopher D. Todd[2], Alejandro Tovar-Mendez[2], Preetinder K. Dhanoa, Natalia Correa-Aragunde, Mary Elizabeth Hoyos, Disa M. Brownfield, Robert T. Mullen, Lorenzo Lamattina, and Joe C. Polacco*

Biochemistry Department, University of Missouri, Columbia, Missouri 65211 (T.F., C.D.T., A.T.-M., M.E.H., J.C.P.); Department of Biology, University of Saskatchewan, Saskatoon, Saskatchewan, Canada S7N 5E2 (C.D.T.); Science Complex, University of Guelph, Guelph, Ontario, Canada N1G 2W1 (P.K.D., R.T.M.); Instituto de Investigaciones Biológicas, Universidad Nacional de Mar del Plata, Mar del Plata 7600, Argentina (N.C.-A., L.L.); Department of Biological Sciences, University of Alberta, Edmonton, Alberta, Canada T6G 2E9 (D.M.B.); and Department of Biophysics and Center of Biotechnology, Universidad Federal do Rio Grande do Sul, Porto Alegre, Rio Grande do Sul, Brazil CEP 91.501–970 (J.C.P.)

Mutation of either arginase structural gene (*ARGAH1* or *ARGAH2* encoding arginine [Arg] amidohydrolase-1 and -2, respectively) resulted in increased formation of lateral and adventitious roots in Arabidopsis (*Arabidopsis thaliana*) seedlings and increased nitric oxide (NO) accumulation and efflux, detected by the fluorogenic traps 3-amino,4-aminomethyl-2′,7′-difluorofluorescein diacetate and diamino-rhodamine-4M, respectively. Upon seedling exposure to the synthetic auxin naphthaleneacetic acid, NO accumulation was differentially enhanced in *argah1-1* and *argah2-1* compared with the wild type. In all genotypes, much 3-amino,4-aminomethyl-2′,7′-difluorofluorescein diacetate fluorescence originated from mitochondria. The arginases are both localized to the mitochondrial matrix and closely related. However, their expression levels and patterns differ: *ARGAH1* encoded the minor activity, and *ARGAH1*-driven β-glucuronidase (*GUS*) was expressed throughout the seedling; the *ARGAH2*::*GUS* expression pattern was more localized. Naphthaleneacetic acid increased seedling lateral root numbers (total lateral roots per primary root) in the mutants to twice the number in the wild type, consistent with increased internal NO leading to enhanced auxin signaling in roots. In agreement, *argah1-1* and *argah2-1* showed increased expression of the auxin-responsive reporter *DR5*::*GUS* in root tips, emerging lateral roots, and hypocotyls. We propose that Arg, or an Arg derivative, is a potential NO source and that reduced arginase activity in the mutants results in greater conversion of Arg to NO, thereby potentiating auxin action in roots. This model is supported by supplemental Arg induction of adventitious roots and increased NO accumulation in *argah1-1* and *argah2-1* versus the wild type.

Nitric oxide (NO) is integral to many plant defense, adaptive, and developmental pathways. In root development, localized increases of NO appear to mediate auxin induction of gravitropic bending in soybean (*Glycine max*; Hu et al., 2005), lateral roots in tomato (*Solanum lycopersicum*; Correa-Aragunde et al., 2004), root hairs in Arabidopsis (*Arabidopsis thaliana*; Lombardo et al., 2006), and adventitious roots in cucumber (*Cucumis sativus*; Pagnussat et al., 2004).

While auxin induces NO accumulation, it is not clear how auxin acts to increase NO or even if this production is enzymatic. For example nonenzymatic production could result from localized auxin-induced increases in acidity (Idam and Newman, 1993) that favor the dismutation of nitrite to nitrate and NO (Stöhr and Ullrich, 2002) or the reduction of nitrite to NO by ascorbate (Beligni et al., 2002). An established enzymatic source of NO in plants is the reduction of nitrite by nitrate reductase (NR), first demonstrated in soybean (Klepper et al., 1979; Dean and Harper, 1986). An NR-null mutant (*nia1 nia2*) of Arabidopsis exhibited less NO production, leading to less elongation of root hairs (Lombardo et al., 2006) and to a lack of abscisic acid-induced stomatal closure (Neill et al., 2003). NO can also be generated from nitrite acting as a terminal acceptor of mitochondrial electron transport. Mitochondria of *nia1 nia2* Arabidopsis leaves pro-

[1] This work was supported by the U.S. Department of Agriculture Cooperative State Research, Education, and Extension Service (grant nos. 2004–38901–02138 and 2006–38901–02138) and by fellowships from the Fulbright and Guggenheim Foundations to J.C.P. and L.L., respectively.

[2] These authors contributed equally to the article.

[3] Present address: Columbia (Missouri) Public Schools, 401 Clinkscales Rd., Columbia, MO 65203.

* Corresponding author; e-mail polaccoj@missouri.edu.

The author responsible for distribution of materials integral to the findings presented in this article in accordance with the policy described in the Instructions for Authors (www.plantphysiol.org) is: Joe C. Polacco (polaccoj@missouri.edu).

[W] The online version of this article contains Web-only data.

[OA] Open Access articles can be viewed online without a subscription.

www.plantphysiol.org/cgi/doi/10.1104/pp.108.121459

duced ^{15}NO from $^{15}NO_2^-$, a production blocked by inhibition of cytochrome electron transport (Modolo et al., 2005). Indeed, addition of nitrite to *nia1 nia2* leaves restored fluorescence by the intracellular NO trap 3-amino,4-aminomethyl-2′,7′-difluorofluorescein diacetate (DAF FM-DA, herewith designated DAF) and restored the hypersensitive response to an incompatible strain of *Pseudomonas syringae* (Modolo et al., 2006). Kaiser's group (Gupta et al., 2005; Kaiser et al., 2007) reported that anaerobic mitochondria of roots of several plants reduced nitrite to NO in the presence of NADH via both the cytochrome and alternative oxidase pathways. They reported that there was no NO production by aerobic leaf mitochondria. In contrast, Modolo et al. (2006) observed NO production by leaf mitochondria in air. No explanation for these different observations has yet been provided.

The *nia1 nia2* mutant produces less NO, in part, because it lacks NR to reduce nitrate sequentially to nitrite and then to NO. Moreover, *nia1 nia2* has drastically lowered nitrite pools for any mitochondrial nitrate-NO conversion. However, Modolo et al. (2006) suggested yet another reason for reduced NO production in *nia1 nia2*: the mutant has only 10% of the free Arg pool of wild-type plants. Leaf infiltration with nitrite or Arg enhanced DAF fluorescence and the hypersensitive response (assayed after 3 h in the dark). The Arg effect could be explained by a plant nitric oxide synthase (NOS), catalyzing the oxidation of Arg to citrulline and NO. Crawford et al. (2006) confirmed an erroneous identification of an Arabidopsis NOS (*AtNOS1*) and renamed it NOA1 (for NO-associated1). However, the *noa1-1* disruption mutant indeed exhibits less NO production and lacks other NO-mediated responses, such as abscisic acid-induced stomatal closure (Guo et al., 2003) and bacterial lipopolysaccharide elicitation of a series of defense genes in the innate immunity response (Zeidler et al., 2004).

Despite the lack of an identified plant *NOS* gene or gene product, several authors have presented data favoring an Arg-NO link. Corpas et al. (2006) identified an Arg-dependent NO-producing activity in extracts of pea (*Pisum sativum*) seedlings. NO was detected by chemiluminescence of its adduct with ozone, and NO production was inhibited by L-NAME (for N^G-nitro-L-Arg methyl ester), an effective inhibitor of animal NOS. The authors cited 12 reports of Arg-dependent production of citrulline or NO, the latter detected by ozone chemiluminescence or by spin-trap electron paramagnetic resonance (Corpas et al., 2007).

Arg, as a precursor of spermine, may stimulate NO accumulation indirectly. The polyamine spermine was reported to stimulate NO efflux in Arabidopsis (Tun et al., 2006). Spermine is produced from putrescine, which can be produced from Arg by either of two routes: (1) via arginase to Orn and then to putrescine via Orn decarboxylase (ODC), or (2) via Arg decarboxylase (ADC) to agmatine and then, via *N*-carbamoylputrescine, to putrescine (Illingworth et al., 2003). Arabidopsis was reported to lack ODC, having only two differentially expressed forms of ADC (Hanfrey et al., 2001; Hummel et al., 2004). If there is no ODC in Arabidopsis, arginase action could diminish the availability of Arg to ADC and the subsequent formation of spermine via pathway 2. Since arginase activity and Arg pools can be considerable, especially during germination and seedling growth (Zonia et al., 1995), mutational elimination of arginase activity can conceivably make more Arg available for the synthesis of spermine and other polyamines.

We report that T-DNA insertion mutation of either of the two arginase structural genes of Arabidopsis results in increased NO accumulation and the propensity to form lateral and adventitious roots, traits under the control of auxin signaling.

RESULTS

Arabidopsis Produces Two Functional Arginases, Each Targeted to the Mitochondrion

Open reading frame (ORF) At4g08870, about 55 kb from the arginase structural gene *ARGAH1* (At4g08900; Krumpelman et al., 1995), encodes paralog ARGAH2, based on the criteria of amino acid identity (86%) and functional expression in yeast (Supplemental Fig. S1). No other arginases were identified in the genome. T-DNA disruption mutant *argah1-1* (see "Materials and Methods") retained about 85% of total arginase activity induced by 6 d after germination (6 DAG) in the progenitor biovar (Columbia [Col-0], or wild type). *argah2-1* seedlings showed a small increase, reaching a plateau at about 4 DAG. Germination, indicated by the arrow (defined as 0 DAG) in Figure 1, occurred about 2 d after the initiation of imbibition at 22°C. The sum of ARGAH1 and ARGAH2 activities in the mutants was roughly equal to that of the wild type during imbibition, germination, and seedling growth.

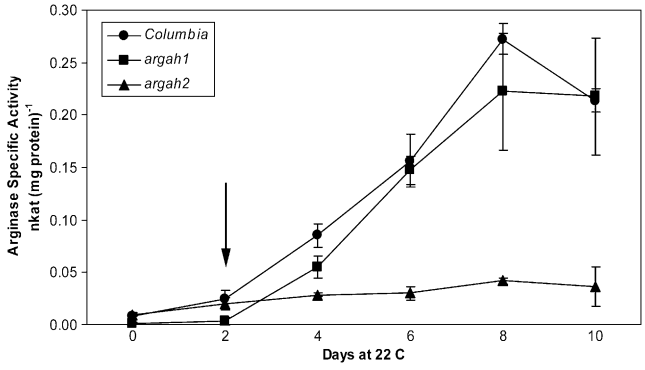

Figure 1. Arginase specific activity during germination and seedling development. Seeds were kept at 4°C in the dark for 2 d prior to transfer to 22°C in the light. Germination occurred in *argah1-1* (squares), *argah2-1* (triangles), and the wild-type (ecotype Col-0; circles) at 2 d (arrow) after transfer to 22°C. Data are expressed in nkat mg^{-1} protein in extracts of total seedlings and are means of three independent biological replicates ± SD.

While the 311 predicted C-terminal amino acids of ARGAH1 and ARGAH2 exhibit 91% identity, only 13 of the 33 N-terminal amino acids are shared by ARGAH1 and ARGAH2. However, both N termini have predicted mitochondrial transit sequences, according to several programs and annotated in the Arabidopsis SubCellular Proteomic Database (Heazlewood et al., 2005). To confirm their predicted mitochondrial location, both proteins were fused at their C termini to the *myc* epitope tag and expressed transiently (via biolistic bombardment) in tobacco (*Nicotiana tabacum*) suspension cultured cells. As shown in Figure 2, immunofluorescence microscopic analysis revealed that both *myc*-tagged ARGAH1 and ARGAH2 colocalized exclusively with the endogenous E1β-subunit of the pyruvate dehydrogenase complex, a well-known mitochondrial matrix marker protein (Luethy et al., 1995). Neither mock transformation nor omission of anti-*myc* and/or anti-E1 antibodies yielded immunofluorescence (data not shown). Neither myc-tagged ARGAH1 nor ARGAH2 was immunodetected in transformed tobacco cells permeabilized with digitonin rather than Triton X-100 (data not shown). Therefore, each protein was actually localized in the mitochondrial interior (matrix), since digitonin permeabilizes only the plasma membrane and only cytosolically exposed antigens are accessible to the applied anti-myc IgGs.

Arginase Isoform Expression in Seedlings

Seedling (3 DAG) expression of *ARGAH1* and *ARGAH2* was examined in transgenic wild-type plants expressing *ARGAH1*::*GUS* and *ARGAH2*::*GUS*, in which *GUS* is under the control of the 1.0- and 1.5-kb genome sequence upstream of the initiator ATG of the respective genes (Brownfield et al., 2008). Expression of each construct showed a unique pattern. Each was expressed in the cotyledon, not surprising in light of an arginase role in the mobilization of reserve nitrogen (Zonia et al., 1995). *ARGAH1*::*GUS* was expressed in the entire cotyledon extending to the mid hypocotyl (Fig. 3A), from which activity was evident in the vasculature almost to the root tip. Although ARGAH2 represents about 75% of total arginase measured in extracts of 3-DAG seedlings (Fig. 1), *ARGAH2*::*GUS* expression was more localized than that of *ARGAH1*::*GUS*. *ARGAH2*-driven GUS showed variability in expression among seedlings. However, the major observed pattern was (from apex to root tip) strong GUS expression in the cotyledons and shoot meristem, lack of expression throughout the hypocotyl, and reappearance of GUS expression in the root vasculature below the hypocotyl-root junction (Fig. 3A). Both constructs were expressed in the root vasculature, although expression of *ARGAH1*::*GUS* extended closer to the root tip.

NO Accumulation, Revealed by DAF Fluorescence, Is Enhanced in Seedlings of *argah1-1* and *argah2-1*

For at least two reasons, inactivation of either structural gene could have localized (tissue or organ) effects on Arg metabolism: (1) *ARGAH2* encodes the major arginase activity (Fig. 1); (2) *ARGAH1*, the structural gene for the minor arginase, is active in tissues in which *ARGAH2* is not expressed (Fig. 3A). To test a possible relationship between Arg breakdown by arginase and NO production from Arg (or Arg derivative), NO accumulation was examined by DAF fluorescence in whole 3-DAG *argah1-1* and *argah2-1* seedlings. Seedlings were grown in ATS medium, preloaded for 30 min with the intracellular NO fluo-

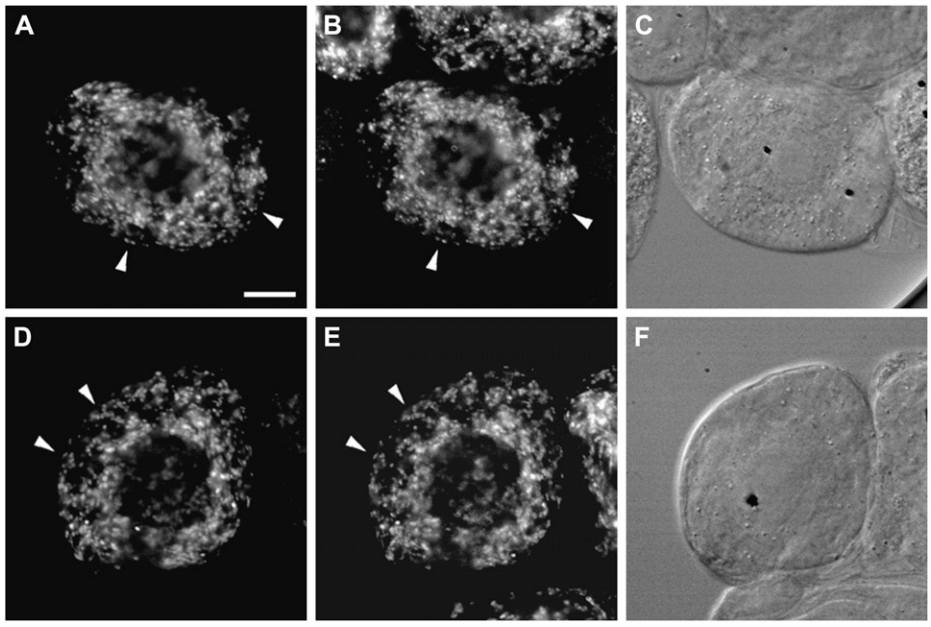

Figure 2. Immunolocalization of ARGAH1 and ARGAH2 in tobacco BY-2 cells. A to F, Cells were transformed with constructs encoding *myc* epitope-tagged ARGAH1 (A–C) or ARGAH2 (D–F), and proteins were detected by immunofluorescence microscopy. Immunodetection of transiently expressed ARGAH1-*myc* (A) was compared with that of endogenous mitochondrial E1β (B) in the same cell. Arrowheads indicate obvious colocalizations. Transiently expressed ARGAH2-*myc* (D) and endogenous E1β (E) were compared in the same manner. C and F show differential interference contrast images of the same cells shown in A/B and D/E, respectively. Bar in A = 10 μm.

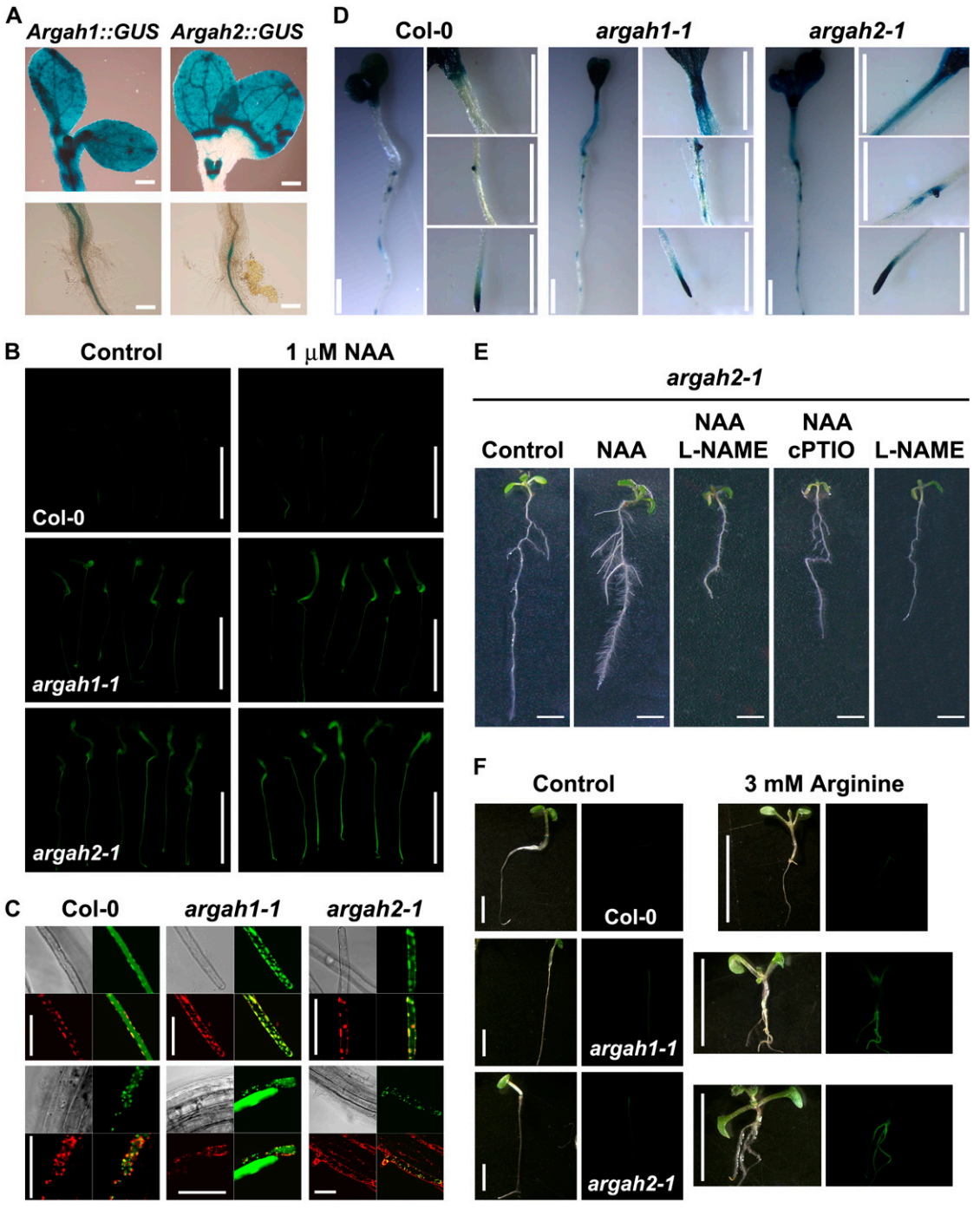

Figure 3. *ARGAH* expression, NO production, and auxin action in the *argah1-1* and *argah2-1* mutants. A, Arginase isoform expression determined by promoter::GUS reporter transgenes in Col-0 seedlings (3 DAG). Seedlings were grown vertically on ATS medium prior to collection for GUS staining. Representative individuals containing ARGAH1::GUS (left) and ARGAH2::GUS (right) reporter constructs are depicted. Staining in the cotyledons and shoot apex (top) and at the root-hypocotyl junction (bottom) illustrates the regions where *ARGAH1* and *ARGAH2* expression show the greatest divergence. Similar staining patterns were observed in independent biological replicates. B, DAF fluorescence of Arabidopsis seedlings exposed to 1 μM NAA. DAF fluorescence images of wild-type (Col-0), *argah1-1*, and *argah2-1* seedlings (3 DAG) without NAA treatment are in the left column, and the corresponding genotypes, after exposure to 1 μM NAA (2 h), are in the right column. C, Dual imaging of DAF and MitoTracker fluorescence in 3-DAG Arabidopsis seedling roots. Top images are of root hairs and bottom images are of the main root. In each image quartet, the subimages are as follows: bright field (top left), DAF fluorescence (top right), MitoTracker fluorescence (bottom left), and merged image of both fluorescence (bottom right). D, Expression of DR5::GUS in *argah1-1* and *argah2-1*. A representative set of seedlings is shown. Each genotype breeds true for the DR5::GUS

rogenic trap DAF, and then exposed for 2 h to 0 or 1 μM naphthaleneacetic acid (NAA).

argah1-1 and *argah2-1* seedlings consistently showed higher DAF fluorescence than wild-type seedlings, especially upon exposure to 1 μM NAA (Fig. 3B). All three genotypes exhibited some root tip fluorescence. There was clearly high fluorescence in the hypocotyl-root junction of *argah1-1*. However, total fluorescence was higher in *argah2-1* overall, with highest signal in cotyledons, upper hypocotyl, and roots. Intriguingly, there was noticeably reduced fluorescence in the lower hypocotyl, in contrast to *argah1-1*, which showed highest fluorescence extending from the hypocotyl-root junction into the mid hypocotyl (Fig. 3B). At 5 μM NAA, there was little difference in fluorescence among the wild type, *argah1-1*, and *argah2-1* (data not shown). These patterns of intracellular DAF fluorescence indicate that the arginase mutants accumulate more NO than the wild type (Col-0), especially when exposed to 1 μM NAA for 2 h.

Root NO Originates, at Least in Part, from the Mitochondrion

Apoplastic (Bethke et al., 2004) and subcellular sources of NO have been described, the latter including the plasma membrane (Stöhr, 2006), peroxisome (Corpas et al., 2004; del Río et al., 2004), plastid (Arnaud et al., 2006), and the mitochondrion (Kaiser et al., 2007; Salgado et al., 2007). We examined subcellular origins of root NO in 3-DAG seedlings preloaded for 30 min with DAF. Fluorescence intensity varied in root hairs and whole root tips, and signal was detected in most of the cell volume. However, by adjusting cell layer and emission detection sensitivity, we found that the highest fluorescence was punctate. DAF-fluorescent foci colocalized with the mitochondrion-specific dye MitoTracker in the wild type, *argah1-1*, and *argah2-1* (Fig. 3C), supporting the mitochondrion as a major NO source in root cells.

Mitochondrial DAF fluorescence was reported by Guo and Crawford (2005). They observed diminished fluorescence in *noa1-1* mitochondria and in wild-type mitochondria treated with the NOS inhibitor L-NAME. In addition, the authors identified a mitochondrial colocalization of NOA1 with MitoTracker. While the data on mitochondrial DAF fluorescence in Figure 3C only reflect the spatial position of the higher DAF signal within the cell, the settings used in each case suggested a higher mitochondrial DAF fluorescence in the arginase disruption mutants than in the wild type (data not shown).

Increased Auxin Signaling in *argah1-1* and *argah2-1* as Determined by *DR5*::*GUS* Expression

NO was reported to mediate auxin induction of lateral roots in tomato (Correa-Aragunde et al., 2004) and adventitious roots in cucumber (Pagnussat et al., 2004). To determine whether increased NO accumulation in the arginase-negative seedlings was correlated with increased auxin signaling, we examined the expression of the *DR5*::*GUS* reporter in *argah1-1* and *argah2-1* seedlings (3 DAG). *DR5*::*GUS* is responsive to increased intracellular auxin levels and/or signaling (Ulmasov et al., 1997). The arginase mutants exhibited increased GUS expression in the lateral root/root boundary, the upper hypocotyls, and the root tip (*argah2-1* > *argah1-1* > wild type). The upper hypocotyl was less intensively stained in *argah1-1* than in *argah2-1*, the mutant lacking the major arginase (Fig. 3D).

Arginase Mutants Have Increased Lateral Root Formation in Response to NAA

Because the arginase mutants had stronger DAF (Fig. 3B) signals than wild-type plants and appeared to have stronger auxin signaling (Fig. 3D), we asked whether auxin-mediated formation of lateral roots was increased in *argah1-1* and *argah2-1*. Seedlings were grown for 3 d on vertical plates and exposed to 0.1 μM NAA for 5 d more. In this experiment, unsupplemented wild-type seedlings produced few lateral roots (length $\geq$ 2 mm) compared with the arginase mutants, which produced more, although the number was small and showed variability among individuals (Table I). All genotypes responded to NAA exposure; however, the arginase mutants produced significantly more lateral roots than the wild type. These results are consistent with an increased capability for NO production in the arginase mutants and, hence, increased response to auxin. In a separate experiment, the NO trap carboxy-2-phenyl-4,4,5,5-tetramethylimidazolinone-3-oxide-1-oxyl (cPTIO) and the animal NOS inhibitor L-NAME both

Figure 3. (*Continued.*)
construct, and for each the pattern of expression of GUS for the whole seedling is shown. To the right of the whole seedling are close-ups of hypocotyls, emerging lateral roots, and root tips (top to bottom). E, Effect of NO depletion and treatment with the animal NOS inhibitor L-NAME on root development in *argah2-1* seedlings exposed to NAA. Seedlings (3 DAG) grown on vertical ATS plates were transferred to fresh medium (control) or to medium containing 0.1 μM NAA, NAA plus 1 mM cPTIO (NO trap), NAA plus 1 mM L-NAME, or L-NAME alone for an additional 5 d. Shown are representative photographs of *argah2-1* seedlings in the different treatments. Quantitative data are given in Fig. 4 for both *argah1-1* and *argah2-1*. F, Arg induction of adventitious roots and DAF fluorescence in *argah1-1* and *argah2-1* seedlings (3 DAG). Seedlings (3 DAG) were grown on vertical plates in ATS medium (control, left column) or in ATS containing 3 mM Arg (right column). Within each column, a bright-field image (left) and a DAF fluorescence image (right) is shown. Bars = 200 μm (A), 5 mm (B), 50 μm (C), 1 mm (D), 5 mm (E), and 3 mm (F).

Table I. *Induction of* lateral roots *(≥2 mm) by the synthetic auxin NAA*

Seedlings (3 DAG) were transferred from ATS medium to ATS control plates or to plates containing ATS with 0.1 mM NAA. Lateral roots were counted after another 5 d. Data presented are mean numbers of lateral roots per seedling from two independent replicates ± SE. For each replicate, at least 20 individual seedlings were assayed. Different superscript letters indicate significant differences between control and NAA-treated wild-type and arginase mutant seedlings ($P < 0.5$).

Treatment	Wild Type	*argah1-1*	*argah2-1*
Control	0.2 ± 0.0^{a}	3.0 ± 0.2^{b}	3.3 ± 0.3^{b}
NAA (0.1 μM)	5.3 ± 0.0^{a}	9.5 ± 0.2^{b}	10.0 ± 0.3^{b}

drastically reduced lateral root numbers in NAA-treated *argah1-1* and *argah2-1* seedlings (Figs. 3E and 4).

Model of Potential Metabolic Sources of NO from Arg, an Arg Derivative (Spermine), or Both

We propose the model shown in Figure 5, in which Arg, or the Arg derivative spermine, or both are sources of NO in Arabidopsis. Tun et al. (2006) reported that spermine induces NO production in Arabidopsis without a lag. By our model, diminished arginase activity in *argah1-1* or *argah2-1* will make more Arg available for NOS activity or for the synthesis of the polyamine, spermine. Arabidopsis lacks ODC (Hanfrey et al., 2001), so the only Arg-to-spermine route is via ADC (Fig. 5).

A prediction of this model is that supplementary Arg should have NO-like effects on root development. Wild-type plants were growth arrested at 5 to 10 mM Arg, either as a supplement to ATS or as sole nitrogen source, and Arg growth inhibition and/or lethality were enhanced in the arginase mutants (data not shown). At 3 mM Arg, however, 3-DAG *argah1-1* and *argah2-1* seedlings exhibited elongated hypocotyls and petioles, curled cotyledons, increased leaf and root thickening, and roots resembling adventitious roots. The wild-type seedling had a much weaker response to Arg: it lacked adventitious roots and root swelling, although there was some lateral root formation and root shortening (Fig. 3F). NO has been reported to mediate auxin induction of adventitious roots in cucumber (Pagnussat et al., 2004) and mung bean (*Vigna radiata*; Huang et al., 2007). Adventitious root formation is under auxin control in Arabidopsis (Sorin et al., 2005). Long petioles and curled cotyledons are also consistent with increased auxin activity in the arginase mutants exposed to Arg. In agreement with increased auxin activity, the root system of Arg-exposed *argah1-1* and *argah2-1* seedlings exhibited high DAF fluorescence (Fig. 3F). While Arg exposure resulted in more DAF fluorescence in wild-type roots, the response was weaker. These observations are consistent with increased conversion of Arg, or an Arg derivative, to NO in the arginase mutants, leading to a high-auxin phenotype.

As a further test of the model, NO efflux was examined in 3-DAG seedlings with the cell-impermeable fluorogenic NO trap diamino-rhodamine-4M (DAR-4M, herewith designated DAR). The model predicts that *argah1-1* and *argah2-1* seedlings will exhibit more NO efflux, from higher internal NO stores (Fig. 3B), than wild-type seedlings. The *argah1-1* and *argah2-1* mutants exhibited approximately twice the DAR signal of the wild type (Fig. 6). In agreement with the model and the results of Tun et al. (2006), spermine further stimulated NO efflux from the wild type. Spermine induced NO efflux from *argah1-1* and *argah2-1* mutants, and efflux was greater than that observed in wild-type seedlings exposed to spermine. These results are consistent with increased NO production in *argah1-1* and *argah2-1* from either Arg or Arg-derived spermine.

DISCUSSION

The arginase mutants *argah1-1* and *argah2-1* accumulate more NO by three criteria: higher DAF fluorescence (internal signal; Fig. 3B), higher DAR fluorescence (NO efflux; Fig. 6), and enhanced lateral root development (Table I), the latter an NAA response

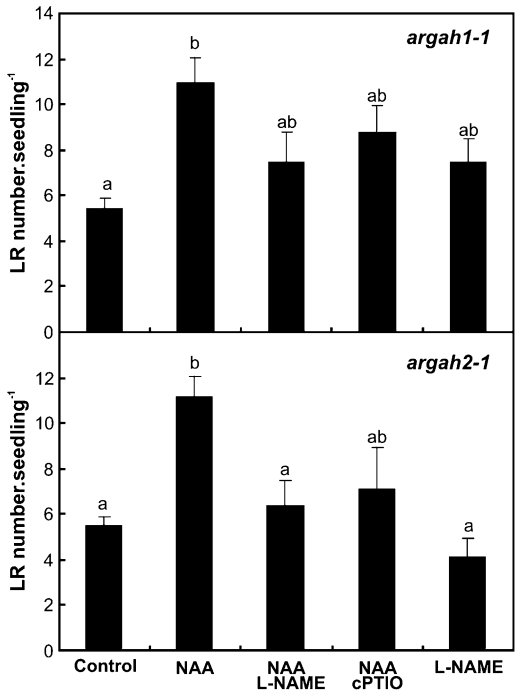

Figure 4. Effects of NO depletion and treatment with the animal NOS inhibitor L-NAME on lateral root number in *argah1-1* and *argah2-1* seedlings exposed to NAA. Seedlings were treated as described in the legend to Table I. The bars represent total lateral roots (LR) per plant (≥2 mm). Shown are averages for a minimum of three independent biological replicates, with four seedlings in each replicate, representing each treatment. Different letters indicate significant differences between treatments (ANOVA test, $P < 0.05$).

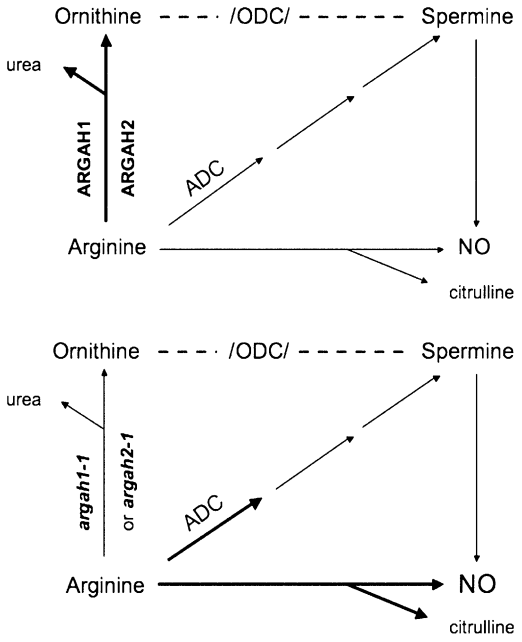

Figure 5. Model of potential metabolic sources of NO from Arg, polyamines (spermine), or both. Arginase action withdraws precursor Arg from NO or polyamine synthesis. Arginase genetic blocks (*argah1-1* or *argah2-1*) result in more available Arg substrate for a NOS-like activity or for ADC. Two further enzyme-catalyzed reactions convert the ADC reaction product, agmatine, to putrescine (Illingworth et al., 2003), a precursor of spermidine, and then to spermine. Arabidopsis lacks an ODC (Hanfrey et al., 2001); hence, the ODC-catalyzed conversion of Orn to spermine, via putrescine and spermidine, is shown as blocked.

mediated by NO and blocked by the NO scavenger cPTIO (Figs. 3E and 4). Our model (Fig. 5) posits that arginase mutants manifest localized increases in available Arg, which can enter into NO-generating reactions directly, or via polyamines (spermine), or via both precursors. We propose greater intramitochondrial Arg availability, which does not necessarily translate to greater pools on a dry weight basis of whole plants or tissues. Corollaries of the model are at least 2-fold. The first is that arginase mutants are primed or more sensitive to the effects of auxin that are mediated by NO. The second is that their ground state of auxin signaling is higher than in the wild type.

Auxin signaling is enhanced by the criterion of increased expression of *DR5*::*GUS* in the arginase mutant backgrounds (Fig. 3D). Also in agreement with the model, supplementary 3 mM Arg had NO-like effects on root development in mutant seedlings, namely, primary root shortening and roots resembling adventitious roots, whereas wild-type seedlings had much weaker responses, no adventitious roots, some lateral root formation, and some root shortening (Fig. 3F). The overall appearance of the arginase-negative seedlings in the presence of 3 mM Arg is strikingly similar to that of the wild type in the presence of the natural auxin precursor indole acetonitrile (Normanly et al., 1997): elongated petioles and curled cotyledons in addition to shortened, thickened, and branched roots. Branched or adventitious root formation is under auxin control in Arabidopsis (Sorin et al., 2005). In cucumber (Pagnussat et al., 2004) and mung bean (Huang et al., 2007), NAA induction of adventitious root formation is mediated by NO. In agreement, 3.0 mM Arg-exposed mutant seedlings accumulated more NO than wild-type seedlings (Fig. 3F). At 5 to 10 mM Arg, wild-type plants were growth restricted, while the arginase mutants generally died shortly after germination (data not shown). A prediction is that a NO trap will reverse some or all of the Arg effects in the mutants. It will also be of interest to define the determinants whereby auxin-induced NO stimulates either lateral root formation (Correa-Aragunde et al., 2006) or adventitious root development.

Another logical test of the model is to examine Arg and polyamine levels. No striking differences were found in whole seedling polyamine content (data not shown). Surprisingly, Arg levels were lower in the mutants (Supplemental Fig. S2). Not shown are other alterations in the amino acid profiles in each mutant. However, without examining cytoplasmic, chloroplastic, and mitochondrial amino acid pools in specific tissues, we can only speculate about how the localized Arg concentrations might be affected. The flux of Arg into various pathways, as opposed to steady-state Arg levels, will have the greatest metabolic impact. We hypothesize that the effective concentration of Arg in the mitochondrion is altered in specific cells of the

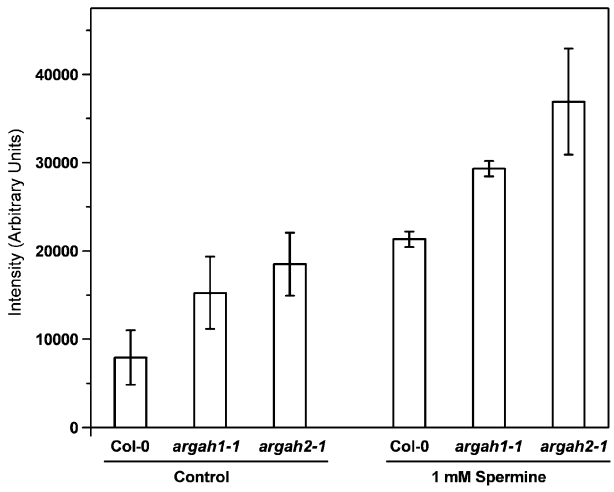

Figure 6. DAR-4M fluorescence determination of NO efflux from seedlings. Seedlings (3 DAG) of the wild type (Col-0), *argah1-1*, and *argah2-1* (20 of each in separate experiments) were incubated with shaking in 2.5 μM DAR-4M, and fluorescence of the supernatant was measured by excitation at 560 nm and emission at 575 nm. Fluorescence (corrected for the DAR-FM background) of *argah1-1* and *argah2-1* was compared with that of similarly corrected Col-0. Determinations were in triplicate, and the average of three independent biological replicates is shown. The spermine treatment was performed once, and determinations were in triplicate.

arginase-negative mutants. A test of this is to use mitochondrial (and other organelle)-specific fluorescent probes for Arg. Arg-induced reporter genes developed in animal cells (Hartenbach et al., 2007) may be modified to elucidate cellular differences in plant Arg content.

Given that Arg is more available for NO generation in the arginase-negative mutants, is the immediate NO precursor Arg, or Arg-derived polyamine(s)? Supplemental spermine, in addition to Arg, enhanced NO evolution, especially in *argah1-1* and *argah2-1* (Fig. 6). In no-spermine controls, enhanced NO evolution from the mutants is consistent with increased availability of spermine, derived from Arg in our model. Exogenous and endogenous polyamines, and polyamine conjugates, have a variety of effects on root development (Couée et al., 2004). In our hands, spermine (up to 1 mM) did not induce lateral root formation, although it shortened the primary roots of all genotypes. In addition, in the presence of spermine, all genotypes appeared somewhat like wild-type plants grown in the presence of indole acetonitrile (Normanly et al., 1997; data not shown).

The model posits a possible NOS-like activity, generating NO directly from Arg. The *nox1* NO-overproducing mutant has a complex phenotype, which includes greatly elevated Arg pools (He et al., 2004). Arg infiltration of detached leaves of the Arabidopsis NR-null mutant *nia1 nia2* (Wilkinson and Crawford, 1993) induced enhanced DAF fluorescence and restored the hypersensitive response to an incompatible strain of *P. syringae* (Modolo et al., 2006; see introduction). Corpas et al. (2006) identified an in vitro Arg-dependent activity in extracts of pea seedlings that produced NO detected by chemiluminescence of its adduct with ozone. The activity was inhibited by L-NAME, an effective inhibitor of animal NOS. The authors cited 12 reports of plant NOS activities, based on Arg-dependent production of citrulline or NO, the latter detected by ozone chemiluminescence or by spin-trap electron paramagnetic resonance (Corpas et al., 2007). Guo and Crawford (2005) observed DAF fluorescence in isolated Arabidopsis mitochondria; the signal was enhanced by Arg and suppressed by L-NAME, an inhibitor of plant (Corpas et al., 2006) as well as animal NOS. To our knowledge, no isolated NOS protein has been reported, nor has a NOS ORF been identified in completely sequenced plant genomes.

NO is produced in response to a large number of stimuli, and the initial NO source in response to those stimuli may vary. Our data indicate that mitochondria, at least in root cells, are significant sources of NO (Fig. 3C). Plastids of Arabidopsis cell culture were reported to exhibit an NO burst in response to iron treatment (Arnaud et al., 2006). NO production in Arabidopsis leaves upon *P. syringae* infection was first accumulated as punctate foci that seemed to be in the plasma membrane or in the cell wall (Chu et al., 2003), although it has been proposed that the main NO source during the interaction of Arabidopsis with *P. syringae* is the reduction of nitrite by the mitochondrial electron transport system (Modolo et al., 2005). The same group later found that the NR-null mutant *nia1 nia2* had low Arg pools and that Arg could mimic nitrite induction of NO release (Modolo et al., 2006). The arginases are mitochondrial (Fig. 2), as is the NOA1 protein (Guo and Crawford, 2005). The authors reported the mitochondria to be a source of NO, as we have found (Fig. 3C). Our model of NO production from Arg (Fig. 5) can be considered in a mitochondrial context whereby arginases, NOA1, and other factors interact, controlling the flux of Arg to NO, Orn, urea, citrulline, and polyamines. It will be important to clarify the roles of inner mitochondrial membrane transporters for basic amino acids (Hoyos et al., 2003; Palmieri et al., 2006) in these fluxes. Any model needs to explain how auxin effects an increase in NO production from Arg in 3-DAG roots. By our model, auxin could increase Arg-dependent NO production by inducing NOS, or polyamine synthesis, or by inhibition of arginase synthesis or activity.

The *ARGAH1* and *ARGAH2* genes are functional by the criteria of arginase promoter-driven GUS expression (Fig. 3A) and functional expression in yeast (Supplemental Fig. S1). Their ORFs share much amino acid similarity, the encoded proteins are targeted to the mitochondrion (Fig. 2), and *argah1-1* and *argah2-1* mutants have measurable arginase activity in seedling extracts (Fig. 1). Why then does each mutant show a phenotype if the activities are at least partially redundant? Three factors lead to an arginase-reduced, or altered, phenotype in the single mutants. (1) *ARGAH1*, the structural gene for the minor arginase, is active in tissues in which *ARGAH2* is not expressed (Fig. 3A). Loss of ARGAH1 in these tissues is effectively an arginase-null localized phenotype. (2) *ARGAH2* encodes the major arginase activity (Fig. 1). In general, elimination of the major ARGAH2 tends to have the greatest effect on fluorescence from DAF (Fig. 3B) and DAR (Fig. 6), indicators of internal and released NO, respectively, on lateral root formation (Table I), and on Arg-induced auxin-like effects and DAF fluorescence (Fig. 3F). (3) *ARGAH1* and *ARGAH2* do not have congruent expression patterns in seedlings (Fig. 1). In pollen, the minor *ARGAH1* is the predominant species. In older plants, *ARGAH2* transcript levels respond much more to methyl jasmonate treatment than *ARGAH1* (Brownfield et al., 2008). *ARGAH1* is greatly induced in roots infected by the clubroot biotrophic protist *Plasmodiophora brassicae*, while there is little or no change in *ARGAH2* (Jubault et al., 2008). We have observed differences in wounding induction of the arginases (C.D. Todd and J.C. Polacco, unpublished data). Finally, the possibility of the formation of mixed multimers of ARGAH1 and ARGAH2 must be considered, so that deletion of one subunit can have effects beyond quantitative reductions in activity. For example, in Arabidopsis, an aminopropyl transferase complex (metabolon) catalyzes the conversion of putrescine to spermine (Panicot et al., 2002), and the

putrescine-to-spermidine reaction is catalyzed by two related spermidine synthases within the complex.

We are continuing attempts to construct *argah1 argah2* double mutant nulls and to optimize the inhibition (Kim et al., 2001) of the remaining arginase in each single mutant.

Recently, Kolbert et al. (2008) concluded that NR action is responsible for auxin-mediated lateral root initiation and NO formation in lateral root primordia in Arabidopsis. We focused on Arg as a potential NO source, holding the nitrate effect constant by providing it in the growth medium (ATS has 9 mM nitrate) and by not targeting NR activity genetically or pharmacologically. Under our conditions, we observed an inhibitory effect of L-NAME on NAA-induced lateral root formation (Figs. 3E and 4), whereas Kolbert et al. (2008) found no effect by the animal NOS inhibitor L-N^G-monomethyl Arg. Making a direct comparison between our data and those of Kolbert et al. (2008) is further complicated by their use of 3-week-old plants while we examined 3-DAG seedlings. They employed L-N^G-monomethyl Arg and we employed L-NAME to inhibit NOS. We provided NAA as an auxin source while they used the indole-3-acetic acid precursor indole butyric acid. We believe that NO is potentially produced from several sources, some of which may influence NO effects downstream.

MATERIALS AND METHODS

Plant Growth

All Arabidopsis (*Arabidopsis thaliana*) plants were in the Col-0 background, the genoptype of the wild type. Unless indicated otherwise, plants were grown sterilely on vertical square (100 × 100 mm) petri dishes. Seeds were surface sterilized in 50% commercial bleach (2.6% sodium hypochlorite final concentration) for 5 min and washed five to six times in sterile distilled water. Seeds were sown on ATS medium (Estelle and Somerville, 1987) with 1% Suc and solidified with 0.8% agar. ATS contains a nitrogen source of 9 mM nitrate. If seeds were not previously vernalized, they were incubated for 2 d at 4°C in the dark. Dishes were then placed in a vertical position and incubated at 25°C under a 16/8-h light/dark cycle. Light was provided by 160-W lamps (Philips F72T12/CW/VHO) at 160 μE m^{-2} s^{-1} (1,600 lux).

ARGAH Cloning and Recovery of Disruption Mutants

The first plant arginase, *ARGAH1* (At4g08900), was cloned earlier from Arabidopsis by functional complementation in yeast (Krumpelman et al., 1995). We identified a second arginase (At4g08870), the only other ortholog in the Arabidopsis genome. The predicted coding region was amplified from total seedling cDNA, cloned into yeast expression vector pFL61, and transformed into an arginase-negative (*car1*) mutant of *Saccharomyces cerevisiae*, in which it conferred the ability to grow with Arg as the sole nitrogen source (Fig. 1). Hence, we designated the At4g08870 ORF as encoding ARGAH2. Our nomenclature differs from that of Chen et al. (2004) for the tomato (*Solanum lycopersicum*) arginases (*Le-Arg-1* and *Le-Arg-2*) to avoid confusion with Arabidopsis ALTERED RESPONSE TO GRAVITY (ARG1; Sedbrook et al., 1999).

T-DNA insertion lines for *argah1* (SALK_057987; Alonso et al., 2003) and *argah2* (SAIL 181_C11; Sessions et al., 2002) were screened for homozygous individuals by PCR of genomic DNA using gene-specific flanking primers. Putative homozygous plants, termed *argah1-1* and *argah2-1*, were confirmed to lack the corresponding *ARGAH* transcript by reverse transcription-PCR (data not shown). They were outcrossed to wild-type plants containing the *DR5*::*GUS* reporter construct (Ulmasov et al., 1997), and homozygous F2 and F3 individuals were used in most studies, although the results were indistinguishable between the original homozyotes and those of the outcross generation.

Assay of Cell-Free Arginase Activity

Whole seedlings were ground in a cooled mortar and pestle with 1.0 mL of ice-cold 10 mM Tris-HCl (pH 9.0) containing1 mM $MnCl_2$, and the homogenate was centrifuged at approximately 14,000*g* for 20 min (4°C) in a 1.5-mL microfuge tube. The supernatant was removed with a drawn out glass Pasteur pipette, avoiding the lipid layer, and assayed for arginase activity essentially as described by King and Gifford (1997).

Immunofluorescence Microscopy of Transiently Expressed *ARGAH1* and *ARGAH2*

The predicted coding regions of *ARGAH1* and *ARGAH2* were amplified by PCR and subcloned into *Xba*I-digested pRTL2/X-myc (Dyer and Mullen, 2001), a plant expression vector that includes the 35S cauliflower mosaic virus promoter, a unique *Xba*I site, and sequences encoding the myc epitope tag (EQKLISEEDL; Fritze and Anderson, 2000), followed by a stop codon. The resulting plasmids were termed pRTL2/ARGAH1-myc and pRTL2/ARGAH2-myc. Tobacco (*Nicotiana tabacum* 'BY-2') suspension-cultured cells were maintained and prepared for biolistic bombardment as described previously (Banjoko and Trelease, 1995). Briefly, transient transformations were performed using 10 μg of plasmid DNA with a biolistic particle delivery system (1000/HE; Bio-Rad Laboratories). Bombarded cells were incubated for 4 h to allow expression and sorting of the introduced gene product(s), then fixed in formaldehyde, incubated with 0.01% (w/v) pectolyase Y-23 (Kyowa Chemical Products), and permeabilized with 0.3% (v/v) Triton X-100 (which permeabilizes both the plasma membrane and organellar membranes) or 25 mg mL^{-1} digitonin (which permeabilizes only the plasma membrane; Sigma-Aldrich; Lee et al., 1997).

Antibody sources were as follows: mouse anti-*myc* antibodies in hybridoma medium (clone 9E10; Princeton University Monoclonal Antibody Facility); rabbit anti-E1 (Luethy et al., 1995); goat anti-mouse Alexa Fluor 488 IgGs (Cedar Lane Laboratories); and goat anti-rabbit rhodamine red-X IgGs (Jackson ImmunoResearch Laboratories). Controls included omitting primary antibodies and mock transformations with pRTL2 alone.

Epifluorescence images of BY-2 cells were acquired using a Zeiss Axioskop 2 MOT epifluorescence microscope (Carl Zeiss) with a Zeiss 63× Plan Apochromat oil-immersion objective. Image capture was performed using a Retiga 1300 CCD camera (Qimaging) and Northern Eclipse 5.0 software (Empix Imaging). All fluorescence images of cells shown in the figures are representative of more than 50 independent (transient) transformations from at least two independent transformation experiments. Figure compositions were generated using Adobe Photoshop CS (Adobe Systems).

NAA-Versus-Genotype Effects on Seedling DAF Fluorescence

Seeds of each genotype (wild type, *argah1-1*, and *argah2-1*) were sown on vertical plates in ATS medium and harvested after 4 d (3 DAG). Seedlings were incubated for 30 min in 15 μM DAF (Invitrogen), given two 10-min washes in loading buffer (5 mM MES, pH 5.7, 0.25 mM KCl, and 1 mM $CaCl_2$), and then incubated for 2 h in 0, 1.0, or 5 μM NAA in loading buffer. Flourescence was determined with a binocular Leica Stereoscope MZFLIII with digital camera (Leica Microsystem). Images were processed with Photoshop 7.0 (Adobe Systems) programs.

Localization of DAF and MitoTracker Fluorescence by Confocal Microscopy

Seedlings (3 DAG) of each genotype were harvested from vertical plates and incubated for 30 min in freshly prepared 15 mM DAF. All treatments and washes were in loading buffer (5 mM MES, pH 5.7, 0.25 mM KCl, and 1 mM $CaCl_2$). Following two 10-min washes, seedlings were incubated for 2 h in 0, 0.5, or 1.0 μM NAA and then for 15 min in freshly prepared 1 μM MitoTracker Red (Molecular Probes-Invitrogen) followed by three 10-min washes. Imaging

of root fluorescence from DAF-FM triazol (excitation, 488 nm; emission measured with a BP 500–550-nm filter) and from MitoTracker Red (excitation, 543 nm; emission measured with an LP 560-nm filter) was carried out with the Zeiss LSM 510 Meta NLO 2-Photon confocal microscope. Images were processed with the LSM Examiner (Zeiss) and Photoshop 7.0 (Adobe Systems) programs.

Measurement of Lateral Root Formation

To determine factors influencing lateral root formation, seeds were sown on vertical plates and at 3 DAG were transferred aseptically to fresh medium containing various additions and grown for 5 d more. Lateral roots (≥2 mm) were counted with the aid of a dissecting microscope. The length of the primary root was measured with the aid of the ImageJ program. Lateral root number was expressed as the number of lateral roots per plant (Table I; Fig. 4) to counter spurious increases in lateral root density due to primary root shortening by NAA. However, not shown were that the effects of auxin on lateral root formation, as determined as lateral root density or lateral roots per plant (which were essentially the same). The statistical analysis software (Fig. 4) was SigmaStat version 3.1 (Systat Software).

Fluorometric Measurement of External NO in 3-DAG Seedlings

The procedure was similar to that of Tun et al. (2006) and employed the cell-impermeable dye DAR-FM developed by Kojima et al. (2000, 2001) for fluorometric determination of NO. Seedlings of the wild type, *argah1-1*, and *argah2-1* were grown as above for the determination of DAF fluorescence, and 20 seedlings (3 DAG) of each genotype were incubated for 4 h in the light in a rotary shaker (60 rpm) in 2 mL of 0.1 M sodium phosphate, pH 7.4, with or without 2.5 μM DAR-4M (EMD Chemicals). Seedlings were discarded, the buffer was clarified by centrifugation, and fluorescence intensity was measured by excitation at 560 nm and emission at 575 nm in an SLM Amingo fluorometer (SLM Instruments). The fluorescence (corrected for the DAR-FM background) of *argah1-1* and *argah2-1* was compared with similarly corrected wild-type levels, taken to be 100%. Determinations were in triplicate.

GUS Staining of Seedlings

Seeds of each genotype (Col-0, *argah1-1*, and *argah2-1*) were sown on vertical plates in ATS medium and harvested after 4 d (3 DAG). Seedlings were incubated for 1 h at −20°C in 90% ice-cold acetone. Acetone was decanted, and enough GUS staining buffer (Jefferson et al., 1987) was added to cover the samples, which were incubated in darkness at 37°C for up to 2 d. Seedlings were rinsed in distilled water, washed in 70% ethanol to remove chlorophyll, and retransferred to distilled water. GUS staining was observed with a binocular Leica Stereoscope MZFLIII and recorded with a digital camera (Leica Microsystem), and images were processed with Photoshop 7.0 (Adobe Systems).

Supplemental Data

The following materials are available in the online version of this article.

Supplemental Figure S1. Arabidopsis arginase expression in yeast.

Supplemental Figure S2. Mol percent (of total free amino acids) in 6-DAG whole seedlings cultured in water.

ACKNOWLEDGMENTS

We thank Jan Miernyk for providing anti-E1β-subunit (pyruvate dehydrogenase complex) antibodies and Tom Guilfoyle and Gretchen Hagen for the DR5::GUS line. The excellent guidance and help of the staff of the University of Missouri Molecular Cytology Core, under Dr. G. Esteban Fernandez, is gratefully acknowledged.

Received April 17, 2008; accepted June 5, 2008; published June 20, 2008.

LITERATURE CITED

Alonso JM, Stepanova AN, Leisse TJ, Kim CJ, Chen H, Shinn P, Stevenson DK, Zimmerman J, Barajas P, Cheuk R, et al (2003) Genome-wide insertional mutagenesis of *Arabidopsis thaliana*. Science **301:** 653–657

Arnaud N, Murgia I, Boucherez J, Briat JF, Cellier F, Gaymard F (2006) An iron-induced nitric oxide burst precedes ubiquitin-dependent protein degradation for *Arabidopsis AtFer1* ferritin gene expression. J Biol Chem **281:** 23579–23588

Banjoko A, Trelease RN (1995) Development and application of an in-vivo plant peroxisome import system. Plant Physiol **107:** 1201–1208

Beligni MV, Fath A, Bethke PC, Lamattina L, Jones RL (2002) Nitric oxide acts as an antioxidant and delays programmed cell death in barley aleurone layers. Plant Physiol **129:** 1642–1650

Bethke P, Badger MR, Jones RL (2004) Apoplastic synthesis of nitric oxide by plant tissues. Plant Cell **16:** 332–341

Brownfield DL, Todd CD, Deyholos MK (2008) Analysis of Arabidopsis arginase gene transcription patterns indicates specific biological functions for recently diverged paralogs. Plant Mol Biol **67:** 429–440

Chen H, McCaig BC, Melotto M, He SY, Howe GA (2004) Regulation of plant arginase by wounding, jasmonate, and the phytotoxin coronatine. J Biol Chem **279:** 45998–46007

Chu ZC, Czymmek KJ, Shapiro AD (2003) Nitric oxide does not trigger early programmed cell death events but may contribute to cell to cell signaling governing progression of the *Arabidopsis* hypersensitive response. Mol Plant Microbe Interact **16:** 962–972

Corpas FJ, Barroso JB, Carreras A, Quirós M, León AM, Romero-Puertas MC, Esteban FJ, Valderrama R, Palma JM, Sandalio LM, et al (2004) Cellular and subcellular localization of endogenous nitric oxide in young and senescent pea plants. Plant Physiol **136:** 2722–2733

Corpas FJ, Barroso JB, Carreras A, Valderrama R, Palma JM, Leon AM, Sandalio LM, del Rio LA (2006) Constitutive arginine-dependent nitric oxide synthase activity in different organs of pea seedlings during plant development. Planta **224:** 246–254

Corpas FJ, Carreras A, Valederrama R, Chaki M, Palma JM, del Rio LA, Barroso JB (2007) Reactive nitrogen species and nitrosative stress in plants. Plant Stress **1:** 37–41

Correa-Aragunde N, Graziano M, Chevalier C, Lamattina L (2006) Nitric oxide modulates the expression of cell cycle regulatory genes during lateral root formation in tomato. J Exp Bot **57:** 581–588

Correa-Aragunde NM, Graziano ML, Lamattina L (2004) Nitric oxide plays a central role in determining lateral root development in tomato. Planta **218:** 900–905

Couée I, Hummel I, Sulmon C, Gouesbet G, El Amranhi A (2004) Involvement of polyamines in root development. Plant Cell Tissue Organ Cult **76:** 1–10

Crawford NM, Galli M, Tischner R, Heimer YM, Okamoto M, Mack A (2006) Response to Zemojtel *et al*: Plant nitric oxide synthase: back to square one. Trends Plant Sci **11:** 526–527

Dean JV, Harper JE (1986) Nitric oxide and nitrous oxide production by soybean and winged bean during the *in vivo* nitrate reductase assay. Plant Physiol **82:** 718–723

del Río LA, Corpas FJ, Barroso JB (2004) Nitric oxide and nitric oxide synthase activity in plants. Phytochemistry **65:** 783–792

Dyer JM, Mullen RT (2001) Immunocytological localization of two plant fatty acid desaturases in the endoplasmic reticulum. FEBS Lett **494:** 44–47

Fritze CE, Anderson TR (2000) Epitope tagging: general method for tracking recombinant proteins. Methods Enzymol **327:** 3–16

Guo FQ, Crawford NM (2005) *Arabidopsis* nitric oxide synthase1 is targeted to mitochondria and protects against oxidative damage and dark-induced senescence. Plant Cell **17:** 3436–3450

Guo FQ, Okamoto M, Crawford NM (2003) Identification of a plant nitric oxide synthase gene involved in hormonal signaling. Science **302:** 100–103

Gupta KJ, Stoimenova M, Kaiser WM (2005) In higher plants, only root mitochondria, but not leaf mitochondria reduce nitrite to NO, in vitro and in situ. J Exp Bot **56:** 2601–2609

Hanfrey C, Sommer S, Mayer MJ, Burtin D, Michael AJ (2001) *Arabidopsis* polyamine biosynthesis: absence of ornithine decarboxylase and the mechanism of arginine decarboxylase activity. Plant J **27:** 551–560

Hartenbach S, Daoud-El Baba M, Weber W, Fussennegger M (2007) An engineered L-arginine sensor of Chlamydia pneumonia enables arginine-adjustable transcription control in mammalian cells and mice. Nucleic Acids Res **35:** e136

He Y, Tang RH, Hao Y, Stevens RD, Cook CW, Ahn SM, Jing L, Yang Z, Chen L, Guo F, et al (2004) Nitric oxide represses the Arabidopsis floral transition. Science **305:** 1968–1971

Heazlewood JL, Tonti-Filippini J, Verboom RE, Millar AH (2005) Combining experimental and predicted datasets for determination of the subcellular location of proteins in Arabidopsis. Plant Physiol **139:** 598–609

Hoyos ME, Palmieri L, Wertin T, Arrigoni R, Polacco JC, Palmieri F (2003) Identification of a mitochondrial transporter for basic amino acids in *Arabidopsis thaliana* by functional reconstitution into liposomes and complementation in yeast. Plant J **33:** 1027–1035

Hu X, Neill SJ, Tang Z, Cai W (2005) Nitric oxide mediates gravitropic bending in soybean roots. Plant Physiol **137:** 663–670

Huang AX, She XP, Huang C, Song TS (2007) The dynamic distribution of NO and NADPH-diaphorase activity during IBA-induced adventitious root formation. Physiol Plant **130:** 240–249

Hummel I, Bourdais G, Gouesbet G, Couee I, Malmberg RL, El Amrani A (2004) Differential gene expression of ARGININE DECARBOXYLASE ADC1 and ADC2 in *Arabidopsis thaliana*: characterization of transcriptional regulation during seed germination and seedling development. New Phytol **163:** 519–531

Idam A, Newman IA (1993) Proton efflux from oat coleoptile cells and exchange with wall calcium after IAA or fusicoccin treatment. Planta **189:** 377–383

Illingworth C, Mayer MJ, Elliott K, Hanfrey C, Walton NJ, Michael AJ (2003) The diverse bacterial origins of the *Arabidopsis* polyamine biosynthetic pathway. FEBS Lett **549:** 26–30

Jefferson RA, Kavanagh TA, Bevan MW (1987) GUS fusions: beta-glucuronidase as a sensitive and versatile gene fusion marker in higher plants. EMBO J **6:** 3901–3907

Jubault M, Hamon C, Gravot A, Lariagon C, Delourme R, Bouchereau A, Manzanares-Dauleux MJ (2008) Differential regulation of root arginine catabolism and polyamine metabolism in clubroot-susceptible and partially resistant Arabidopsis genotypes. Plant Physiol **146:** 2008–2019

Kaiser WM, Gupta KJ, Planchet E (2007) Higher plant mitochondria as a source for NO. *In* L Lamattina, JC Polacco, eds, Nitric Oxide in Plant Growth. Plant Cell Monographs, Vol 6. Springer, Berlin, pp 1–14

Kim NN, Cox DJ, Baggio RF, Emig FA, Mistry SK, Harper SL, Speicher DW, Morris SM Jr, Ash DE, Traish A, et al (2001) Probing erectile function: S-(2-boronoethyl)-L-cysteine binds to arginase as a transition state analogue and enhances smooth muscle relaxation in human penile corpus cavernosum. Biochemistry **40:** 2678–2688

King JE, Gifford DJ (2004) Amino acid utilization in seeds of loblolly pine during germination and early seedling growth. 1. Arginine and arginase activity. Plant Physiol **113:** 1125–1135

Klepper L (1979) Nitric oxide (NO) and nitrogen dioxide (NO_2) emissions from herbicide-treated soybean plants. Atmos Environ **13:** 537–542

Kojima H, Hirotani M, Nakatsubo N, Kikuchi K, Urano Y, Higuchi T, Hirata Y, Nagano T (2001) Bioimaging of nitric oxide with fluorescent indicators based on the rhodamine chromophore. Anal Chem **73:** 1967–1973

Kojima H, Hirotani M, Urano Y, Kikuchi K, Higuchi T, Nagano T (2000) Fluorescence indicators for nitric oxide based on rhodamine chromophore. Tetrahedron Lett **41:** 69–72

Kolbert Z, Bartha B, Erdei L (2008) Exogenous auxin-induced NO synthesis is nitrate reductase-associated in *Arabidopsis thaliana* root primordia. J Plant Physiol **165:** 967–975

Krumpelman PM, Freyermuth SK, Cannon JC, Fink GR, Polacco JC (1995) Nucleotide sequence of *Arabidopsis thaliana* arginase expressed in yeast. Plant Physiol **107:** 1479–1480

Lee MS, Mullen RT, Trelease RN (1997) Oilseed isocitrate lyases lacking their essential type 1 peroxisomal targeting signal are piggybacked to glyoxysomes. Plant Cell **9:** 185–197

Lombardo MC, Graziano ML, Polacco JC, Lamattina L (2006) Nitric oxide functions as a positive regulator of root hair development. Plant Signaling and Behavior **1:** 28–33

Luethy MH, David NR, Elthon TE, Miernyk JA, Randall DD (1995) Characterization of a monoclonal-antibody recognizing the E1-alpha subunit of plant mitochondrial pyruvate-dehydrogenase. J Plant Physiol **145:** 443–449

Modolo LV, Augusto O, Almeida IMG, Magalhaes JR, Oliveira HC, Salgado I (2005) Nitrite as the major source of nitric oxide production by *Arabidopsis thaliana* in response to *Pseudomonas syringae.* FEBS Lett **579:** 3814–3820

Modolo LV, Augusto O, Almeida IMG, Pinto-Maglio CAF, Oliveira HC, Seligman K, Salgado I (2006) Decreased arginine and nitrite levels in nitrate reductase-deficient *Arabidopsis thaliana* plants impair nitric oxide synthesis and the hypersensitive response to *Pseudomonas syringae.* Plant Sci **171:** 34–40

Neill SJ, Desikan R, Hancock JT (2003) Nitric oxide signalling in plants. New Phytol **159:** 11–35

Normanly J, Grisafi P, Fink GR, Bartel B (1997) *Arabidopsis* mutants resistant to the auxin effects of indole-3-acetonitrile are defective in the nitrilase encoded by the *NIT1* gene. Plant Cell **9:** 1781–1790

Pagnussat CG, Lanteri ML, Lombardo MC, Lamattina L (2004) Nitric oxide mediates the indole acetic acid induction activation of a mitogen-activated protein kinase cascade involved in adventitious root development. Plant Physiol **135:** 279–286

Palmieri L, Todd CD, Arrigoni R, Hoyos ME, Santoro A, Polacco JC, Palmieri F (2006) *Arabidopsis* mitochondria have two basic amino acid transporters with partially overlapping specificities and differential expression in seedling development. Biochim Biophys Acta **1757:** 1277–1283

Panicot M, Minguet EG, Ferrando A, Alcázar R, Blázquez MA, Carbonell J, Altabella T, Koncz C, Tiburcio AF (2002) A polyamine metabolon involving aminopropyl transferase complexes in *Arabidopsis.* Plant Cell **14:** 2539–2551

Salgado I, Modolo LV, Ohara A, Braga MR Oliveira HC (2007) Mitochondrial nitric oxide synthesis during plant-pathogen interactions: role of nitrate reductase in providing substrates. *In* L Lamattina, JC Polacco, eds, Nitric Oxide in Plant Growth. Plant Cell Monographs, Vol 6. Springer, Berlin, pp 239–254

Sedbrook JC, Chen RJ, Masson PH (1999) ARG1 (altered response to gravity) encodes a DnaJ-like protein that potentially interacts with the cytoskeleton. Proc Natl Acad Sci USA **96:** 1140–1145

Sessions A, Burke E, Presting G, Aux G, McElver J, Patton D, Dietrich B, Ho P, Bacwaden J, Ko C, et al (2002) A high-throughput *Arabidopsis* reverse genetics system. Plant Cell **14:** 2985–2994

Sorin C, Bussell JD, Camus I, Ljung K, Kowalczyk M, Geiss G, McKhann H, Garcion C, Vaucheret H, Sandberg G, et al (2005) Auxin and light control of adventitious rooting in *Arabidopsis* require ARGONAUTE1. Plant Cell **17:** 1343–1359

Stöhr C (2006) Nitric oxide: a product of plant nitrogen assimilation. *In* L Lamattina, JC Polacco, eds, Nitric Oxide in Plant Growth. Plant Cell Monographs, Vol 6. Springer, Berlin, pp 15–34

Stöhr C, Ullrich WR (2002) Generation and possible roles of NO in plant roots and their apoplastic space. J Exp Bot **53:** 2293–2303

Tun NN, Santa-Catarina C, Begum T, Silveira V, Handro W, Floh EIS, Scherer GFE (2006) Polyamines induce rapid biosynthesis of nitric oxide (NO) in *Arabidopsis thaliana* seedlings. Plant Cell Physiol **47:** 346–354

Ulmasov T, Murfett J, Hagen G, Guilfoyle TJ (1997) Aux/IAA proteins repress expression of reporter genes containing natural and highly active synthetic auxin response elements. Plant Cell **9:** 1963–1971

Wilkinson JQ, Crawford NM (1993) Identification and characterization of a chlorate resistant mutant of Arabidopsis with mutations in both NIA1 and NIA2 nitrate reductase structural genes. Mol Gen Genet **239:** 289–297

Zeidler D, Zähringer U, Gerber I, Dubery I, Hartung T, Bors W, Hutzler P, Durner J (2004) Innate immunity in *Arabidopsis thaliana*: Lipopolysaccharides activate nitric oxide synthase (NOS) and induce defense genes. Proc Natl Acad Sci USA **101:** 15811–15816

Zonia LE, Stebbins NE, Polacco JC (1995) Essential role of urease in germination of nitrogen-limited *Arabidopsis thaliana* seeds. Plant Physiol **107:** 1097–1103